Journal of the Korean Chemical Society
1995, *Vol. 39, No. 6*
Printed in the Republic of Korea

Li_2FeMoO_4Cl의 결정구조와 Fe 및 Mo의 전자구조 연구

崔珍鎬* · 朴南圭 · 張舜浩† · 朴鎭浩†
서울대학교 자연과학대학 화학과, †전자통신연구소
(1995. 2. 27 접수)

Electronic Structure of Iron and Molybdenum in Li_2FeMoO_4Cl and Its Crystal Symmetry

Jin-Ho Choy*, Nam-Gyu Park, Soon-Ho Chang†, and Hyung-Ho Park†
Department of Chemistry, Seoul National University, Seoul 151-742, Korea
†Research Department, Electronics and Telecommunication Research Institute, Daejeon 305-606, Korea
(Received February 27, 1995)

요 약. 전기화학적으로 리튬이온을 $FeMoO_4Cl$ 격자내에 층간삽입시킨 Li_xFeMoO_4Cl 화합물은 X-선 회절분석 및 정전류 방전 실험 결과 $1 \le X \le 2$ 영역에서 단사정계로 결정화되었다. X-선 광전자 분광분석 연구결과, $0 \le X \le 1$ 영역에서는 리튬이온의 층간삽입시 Fe(III) 이온이 Fe(II) 이온으로 환원되었으며 이때 결정구조는 정방정계에서 단사정계로 전이되었다. 반면, $1 \le X \le 2$ 영역에서는 Mo(VI) 이온이 낮은 산화상태로 환원되었고, 결정계 전이나 Fe(II) 이온의 환원은 관찰되지 않았다. Mo의 3d X-선 광전자 스펙트럼을 가우스 함수를 이용하여 deconvolution한 결과, Mo(VI), Mo(V) 및 Mo(IV)에 해당하는 세 종류의 피크를 분리해 낼 수 있었다. 이와 같이 Mo가 혼합 원자가 상태로 존재하는 이유는 리튬이 층간삽입됨에 따라 생성된 Mo(V)의 일부가 Mo(IV)와 Mo(VI)로 disproportionation되기 때문이다.

ABSTRACT. Lithium intercalates, Li_xFeMoO_4Cl ($1 \le X \le 2$) prepared by electrochemical lithiation of $FeMoO_4Cl$, crystallizes in monoclinic structure for all x values as revealed by x-ray diffraction and galvanostatic discharge experiments. According to the x-ray photoelectron spectroscopic study, Fe(III) is at first reduced to Fe(II) upon lithium intercalation with the x domain of $0 \le X \le 1$, where the crystal symmetry is changed from tetragonal to monoclinic. On the other hand, Mo(VI) is reduced to lower valent state upon further lithium intercalation ($1 \le X \le 2$), where no crystal symmetry transformation and reduction of Fe(II) to lower valent state are observed. The Mo 3d spectrum for Li_2FeMoO_4Cl appears as a complex shape, but can be deconvoluted into the three sets of the doublet on the basis of Gaussian function, those which correspond to Mo(VI), Mo(V) and Mo(IV) states, respectively. The mixed valent states of molybdenum after further lithiation may be due to a competitive reaction between the formation of Mo(V) and its disproportionation to Mo(IV) and Mo(VI).

INTRODUCTION

Much interest in the study of the structural and electronic properties of lithium intercalation compounds has been generated because of their potential application as cathode materials in rechargeable electrochemical cells. Recently we have reported on synthesis, crystal structure, magnetic and spectroscopic properties for the lithium intercalated Li_xFeMoO_4Cl with $0 \le X \le 1$ and found that the crystal symmetry was changed from tetragonal ($FeMoO_4Cl$) to monoclinic ($LiFeMoO_4Cl$) and that in XPS study only the binding energy of the 2p electrons for iron was changed from 711.0 eV (Fe $2p_{3/2}$ for $FeMoO_4Cl$) to 710.2 eV (Fe $2p_{3/2}$ for $LiFeMoO_4Cl$) due to the reduction of Fe(III) to Fe(II) upon lithium intercalation.[1~4]

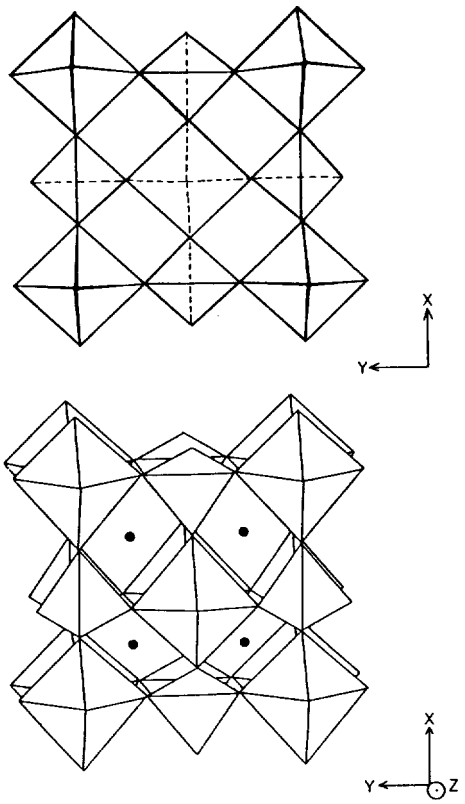

Fig. 1. A section of the polyhedra linking in $FeMoO_4Cl$ layer represented by corner sharing MoO_4 tetrahedral and FeO_4Cl square pyramids on the XY plane (top). Perspective view of the polyhedra linking in Li_2FeMoO_4Cl with two stacked layers. The interlayer "octahedral" sites are represented as (●), which is identical with the Li position (bottom).

The pristine material, $FeMoO_4Cl$, has vacant octahedral sites in the interlayer space composed of four oxygen and two chlorine atoms (*Fig.* 1) and two reducible cations such as Fe(III) and Mo(VI) within the sheet. According to our previous crystal structure study on $LiFeMoO_4Cl$, we have found that two of the four vacant octahedral sites are occupied by lithium ions.[1] It is therefore expected that the two more Li^+ ions could be intercalated into the two remaining vacant sites of the interlayer of $LiFeMoO_4Cl$ without any reconstruction of its crystal structure.

In this report, an attempt was made to synthesize a further lithiated phase Li_xFeMoO_4Cl ($x \cong 2$) and X-ray photoelectron spectroscopic study has been carried out to understand the evolution of electronic structure of transition elements upon lithium intercalation.

EXPERIMENTAL

$FeMoO_4Cl$ has been prepared in the same manner as described previously.[3] The mixture of Fe_2O_3, MoO_3 and $FeCl_3$ (molar ratio 1 : 3 : 1.05) was heated in a sealed Pyrex tube at about 380 ℃ for several days according to the chemical vapor transport (CVT) technique. Electrochemical lithiation has been carried out with a two-electrode cell of the form:

$Li/LiClO_4$ in PC/$FeMoO_4Cl$+ketjen black,

The cathode consists of finely ground $FeMoO_4Cl$ mixed with ketjen black (up to 30% by weight) to enhance the electronic conductivity. $LiClO_4$ solution (1M) in propylene carbonate (PC) absorbed in glass-wool disc was used as the liguid electrolyte. Cell was galvanostatically discharged and charged at constant current densities of 30~100 μA /cm^2 under argon atmosphere.

X-ray powder diffraction data have been obtained by multi channel analyzer where Cu-Kα (λ= 1.5405 Å) was used. X-ray photoelectron spectra using a Mg-Kα radiation (1253.6 eV) have been recorded on an ESCALAB/200R V.G. Scientific X-ray Photoelectron Spectrometer equipped with Micro-PDP 11/53 computer system. The base pressure was maintained in the ~10^{-9} torr throughout all operation. Instrumental work function was calibrated by the Au ($4f_{7/2}$) binding energy at 83.8 eV. The powder sample was pressed into pellet, mounted on the sample holder which was covered with a gold sheet and put into the chamber without exposure to air. All binding energies were corrected with the carbon 1s line (284.4 eV).[4]

RESULTS AND DISCUSSION

The electrochemical lithium intercalation-deintercalation has been realized either by continuous discharge-charge under constant current density as shown in *Fig.* 2. The curve shape in the domain between $FeMoO_4Cl$ and $LiFeMoO_4Cl$ is completely

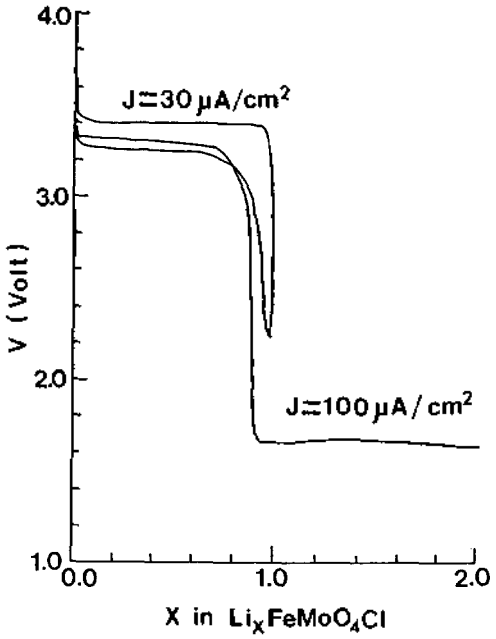

Fig. 2. Cell voltage variation *vs.* the amount of intercalation in $FeMoO_4Cl$ according to the discharge depth value.

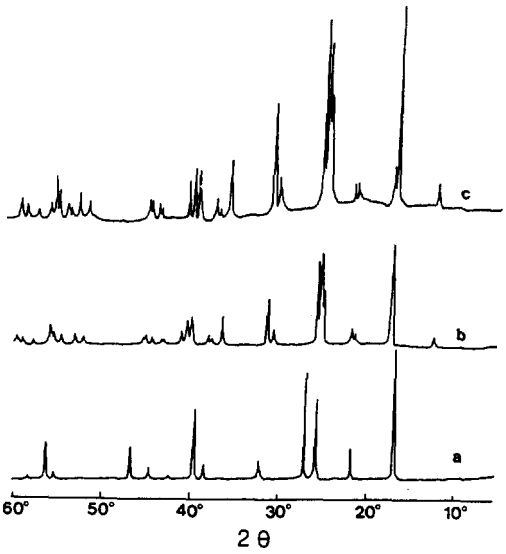

Fig. 3. X-ray diffraction patterns for (a) $FeMoO_4Cl$, (b) $LiFeMoO_4Cl$ and (c) Li_2FeMoO_4Cl.

reversible, and the small voltage difference indicates a reduced polarization. Though an effort has been made to perform the discharge-charge experiment in the x domain of $0 \leq X \leq 2$ by the open circuit voltage method, the open circuit voltage diagram could not be obtained due to the large polarization effect in the x domain of $1 \leq X \leq 2$. The constant potential of discharge curve for $x>1$ underlines the formation of the two phases without any structural transformation, and which is in turn confirmed by the XRD analysis as shown in *Fig.* 3.

The structure of a further lithiated phase with nominal composition Li_2FeMoO_4Cl is similar to that of $LiFeMoO_4Cl$ and closely related to that of $FeMoO_4Cl$. According to the powder X-ray diffraction pattern (*Fig.* 3(c)), the crystal symmetry of Li_2FeMoO_4Cl is found to be monoclinic with lattice parameters $a=7.042(2)$, $b=6.906(1)$, $c=5.049(1)$ Å and $\beta=91.37°$. The indexed XRD pattern for Li_2FeMoO_4Cl is given in *Table* 1. Even two moles of lithium are intercalated, the crystallinity is still retained, which might be due to the fact that the vacant octahedral sites in the lattice allowed are exactly consistent with four Li^+ ions per $FeMoO_4Cl$ unit cell ($z=2$), as shown in *Fig.* 1.

In order to investigate whether the distribution of lithium ions has an influence on the X-ray intensity or not, the theoretical X-ray diffraction intensity for two lithiated phases $LiFeMoO_4Cl$ and Li_2FeMoO_4Cl has been calculated. On the basis of monoclinic unit cell of $LiFeMoO_4Cl$ with space group $P2_1/m$ determined by X-ray[1] and neutron powder diffraction data,[5] lithium ions in $LiFeMoO_4Cl$ ($z=2$) are placed in the two crystallographic interlayer octahedral sites at (0.26, 0.25, 0.25) and (0.77, 0.75, 0.25), and those of Li_2FeMoO_4Cl ($z=2$) are placed at (0.26, 0.25, 0.25), (0.26, 0.75, 0.25), (0.77, 0.75, 0.25) and (0.77, 0.25, 0.25), where iron ions occupy the eight corners of the cell and one more occupies the center of the cell. As expected, the calculated X-ray intensity patterns between $LiFeMoO_4Cl$ and Li_2FeMoO_4Cl can not be distinguished even though lithium ions occupy all the octahedral sites remained in the $LiFeMoO_4Cl$ lattice, which is surely due to the small values of the atomic scattering factor of lithium ion.

The (00l) peaks of the lithiated phase are shifted to the higher angle than those of the pristine $FeMoO_4Cl$, which indicates a strong electrostatic

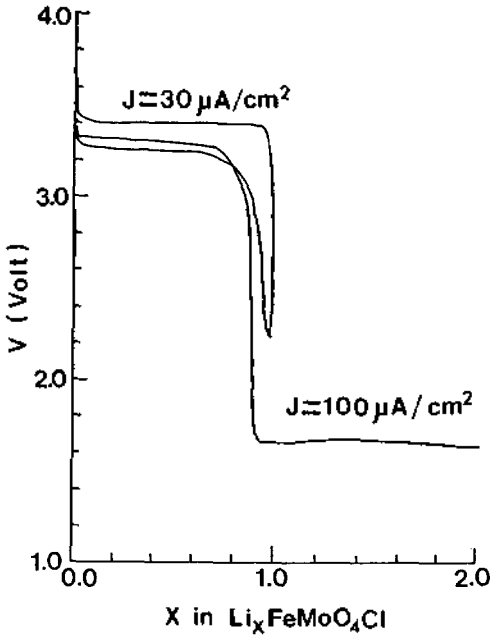

Fig. 2. Cell voltage variation *vs.* the amount of intercalation in $FeMoO_4Cl$ according to the discharge depth value.

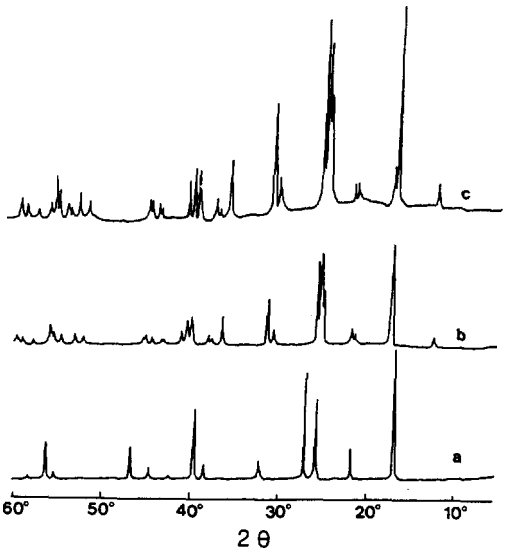

Fig. 3. X-ray diffraction patterns for (a) $FeMoO_4Cl$, (b) $LiFeMoO_4Cl$ and (c) Li_2FeMoO_4Cl.

reversible, and the small voltage difference indicates a reduced polarization. Though an effort has been made to perform the discharge-charge experiment in the x domain of $0 \leq X \leq 2$ by the open circuit voltage method, the open circuit voltage diagram could not be obtained due to the large polarization effect in the x domain of $1 \leq X \leq 2$. The constant potential of discharge curve for $x>1$ underlines the formation of the two phases without any structural transformation, and which is in turn confirmed by the XRD analysis as shown in *Fig.* 3.

The structure of a further lithiated phase with nominal composition Li_2FeMoO_4Cl is similar to that of $LiFeMoO_4Cl$ and closely related to that of $FeMoO_4Cl$. According to the powder X-ray diffraction pattern (*Fig.* 3(c)), the crystal symmetry of Li_2FeMoO_4Cl is found to be monoclinic with lattice parameters $a=7.042(2)$, $b=6.906(1)$, $c=5.049(1)$ Å and $\beta=91.37°$. The indexed XRD pattern for Li_2FeMoO_4Cl is given in *Table* 1. Even two moles of lithium are intercalated, the crystallinity is still retained, which might be due to the fact that the vacant octahedral sites in the lattice allowed are exactly consistent with four Li^+ ions per $FeMoO_4Cl$ unit cell ($z=2$), as shown in *Fig.* 1.

In order to investigate whether the distribution of lithium ions has an influence on the X-ray intensity or not, the theoretical X-ray diffraction intensity for two lithiated phases $LiFeMoO_4Cl$ and Li_2FeMoO_4Cl has been calculated. On the basis of monoclinic unit cell of $LiFeMoO_4Cl$ with space group $P2_1/m$ determined by X-ray[1] and neutron powder diffraction data,[5] lithium ions in $LiFeMoO_4Cl$ ($z=2$) are placed in the two crystallographic interlayer octahedral sites at (0.26, 0.25, 0.25) and (0.77, 0.75, 0.25), and those of Li_2FeMoO_4Cl ($z=2$) are placed at (0.26, 0.25, 0.25), (0.26, 0.75, 0.25), (0.77, 0.75, 0.25) and (0.77, 0.25, 0.25), where iron ions occupy the eight corners of the cell and one more occupies the center of the cell. As expected, the calculated X-ray intensity patterns between $LiFeMoO_4Cl$ and Li_2FeMoO_4Cl can not be distinguished even though lithium ions occupy all the octahedral sites remained in the $LiFeMoO_4Cl$ lattice, which is surely due to the small values of the atomic scattering factor of lithium ion.

The (00l) peaks of the lithiated phase are shifted to the higher angle than those of the pristine $FeMoO_4Cl$, which indicates a strong electrostatic

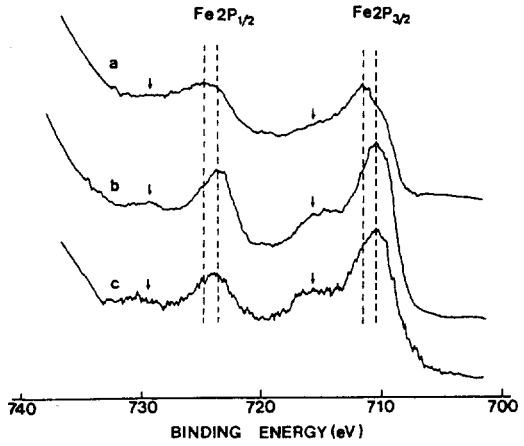

Fig. 4. Fe 2p XPS spectra of (a) $FeMoO_4Cl$, (b) $LiFeMoO_4Cl$ and (c) Li_2FeMoO_4Cl after Ar ion sputtering for several min. Satellite peaks are indicated by arrows.

most no change in the XPS lines for O 1s and Cl 2p except for Fe 2p and Mo 3d before and after lithiation. In the case of $LiFeMoO_4Cl$, only the BE's of Fe 2p core lines were changed due to the reduction of Fe(III) to Fe(II), whereas the noticeable change in Li_2FeMoO_4Cl occurs in Mo 3d core lines as well as Fe 2p core lines. The changes in BE of Fe 2p core lines for Li_2FeMoO_4Cl are shown in *Fig.* 4(c). The BE's of Fe $2p_{1/2}$ and $2p_{3/2}$ core electrons for $FeMoO_4Cl$ are estimated as 724.3 eV and 711.0 eV, respectively, whereas those of Fe 2p core lines for Li_2FeMoO_4Cl are shifted to lower binding energy by −1 eV as those for $LiFeMoO_4Cl$, which indicates a decrease in the oxidation state of iron (Fe(III) → Fe(II)).

It is found that 2p XPS spectra of the compounds containing 3d-group transition metals (Fe, Co, Ni, Cu, *etc.*) are particularly difficult to analyze because of a steeply rising background and broadening line widths caused by multiplet splitting and shake-up phenomena.[6] Multiplet splitting of core-level peaks can occur when the system has unpaired electrons in the valence levels. And this effect causes broadening (with asymmetry) in both $2p_{1/2}$ and $2p_{3/2}$ peaks. The multiple electron transitions producing shake-up process are now similarly well understood. Very strong shake-up satellites are observed for certain transition metal and rare

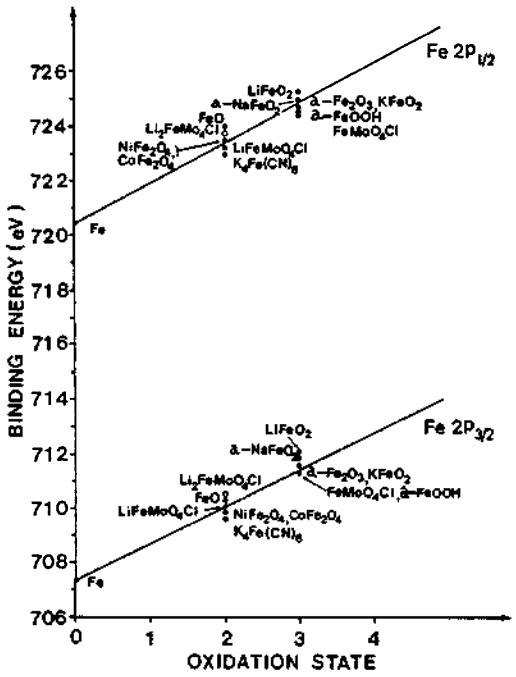

Fig. 5. Fe($2p_{1/2}$-$2p_{3/2}$) binding energies as a function of oxidation state. Data are available from references 4, and 6~8 (●) and this work (○).

earth compounds which have unpaired electrons in 3d or 4f shells, respectively.

Fe 2p spectra, as in *Fig.* 4, show the parent doublet peaks, which are broadened (ca. 3.3 eV) with satellites. When applying the above considerations to the present system, it can be deduced that Fe(III) ion in $FeMoO_4Cl$ and Fe(II) one in Li_xFeMoO_4Cl ($x=1$, 2) are in high spin (^6S) and (^5D) states with 5 and 4 unpaired valence electrons, respectively. The BE's for Fe $2p_{1/2}$ and $2p_{3/2}$ are plotted with respect to the oxidation states of iron for various iron-containing compounds along with $FeMoO_4Cl$ and its lithium derivatives (*Fig.* 5). As expected, an increase in oxidation state provides an increase in binding energy. And it is found that the Fe 2p BE's of 723.7 eV (Fe $2p_{1/2}$) and 710.4 eV (Fe $2p_{3/2}$) in Li_2FeMoO_4Cl corresponds to the Fe(II) state. At first, it is thought that Mo(VI) in the lattice might be reduced to Mo(V), since no XPS evidence of reduction from Fe(II) to Fe(0) in Li_2FeMoO_4Cl was observed upon further lithiation.

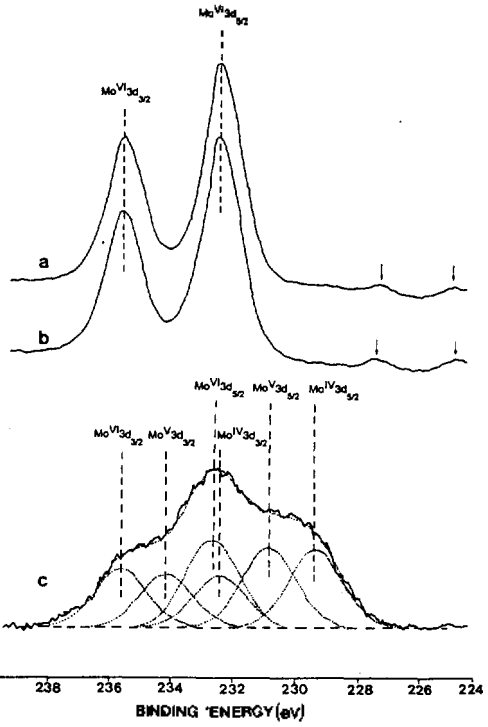

Fig. 6. Mo 3d XPS spectra of (a) $FeMoO_4Cl$, (b) $LiFeMoO_4Cl$ and (c) Li_2FeMoO_4Cl after Ar ion sputtering for several min. X-ray satellite peaks are indicated by arrows. The dotted lines in figure c represent the result of computer fit according to Gaussian function: (−) experimental data, (···) computer fit.

Table 4. Binding energies (eV) and the fitting parameters of Mo 3d spectrum for Li_2FeMoO_4Cl

	BE of $3d_{5/2}$	BE of $3d_{3/2}$	fwhm (eV)	σ^a	$I_{5/2}{}^a$	$I_{3/2}{}^a$
Mo(VI)	232.62	235.57	2	0.85	19.4	12.9
Mo(V)	230.80	234.10	2	0.85	17.6	11.7
Mo(IV)	229.30	232.35	2	0.85	17.2	11.5

[a]Parameters for Gaussian equation as:

$$f(x)=I_n \frac{1}{\sqrt{(2\pi)\sigma}} \exp\frac{(x-x_0)^2}{2\sigma^2}, \text{ where } I_{5/2}=1.5\ I_{3/2}.$$

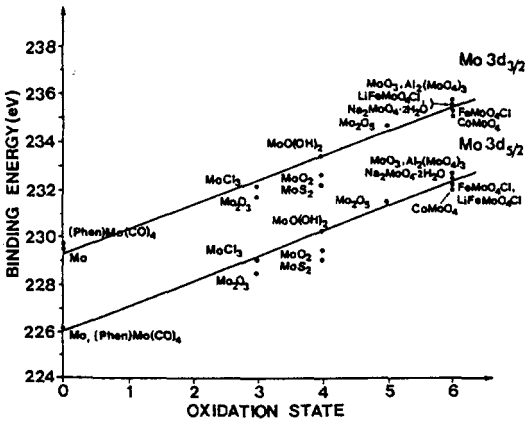

Fig. 7. Mo ($3d_{3/2}$-$3d_{5/2}$) binding energies as a function of oxidation state. Data are available from references 4, and 10−13.

Mo 3d spectra for both $FeMoO_4Cl$ and $LiFeMoO_4Cl$ show the same shape (full width at half maximum (FWHM)=1.6 eV for $FeMoO_4Cl$ and $LiFeMoO_4Cl$) with no satellite lines except x-ray satellites 8 eV lower than the main XPS lines and BE's indicating that Mo(VI) species is not reduced even after 1 mol of lithium intercalation. On the other hand, the Mo 3d spectrum for Li_2FeMoO_4Cl (*Fig.* 6(c)) is rather complex in shape due to the superimposed doublets of several oxidation states. In the curve fitting procedure, a linear background is assumed and the line shape is derived from the analysis of the Mo(VI) doublet in the $FeMoO_4Cl$ spectrum. The doublet was well reproduced by Gaussian lines. The FWHM used in the fitting is by 25% higher than that of the Mo 3d line for $FeMoO_4Cl$ spectrum (1.6 eV). The intensity between Mo $3d_j$ lines (j=3/2 and 5/2) for $FeMoO_4Cl$ is observed clearly in the ratio of 2 : 3, which is consistent with the expected intensity of the doublet peaks given by the ratio of their respective degeneracy $(2j+1)$.[9]

The BE's and the fitting parameters are listed in *Table* 4. The best computer fit for the Mo 3d envelope is shown in *Fig.* 6(c), and the spectrum could be deconvoluted into three sets of the doublet. The BE's of Mo $3d_{3/2}$ and $3d_{5/2}$ electrons *vs.* the oxidation states are also plotted for various molybdenum containing compounds with different oxidation states (*Fig.* 7). As in the iron case the BE's of Mo 3d electrons increase as the oxidation state become more positive. The BE value for molybdenum found in Li_2FeMoO_4Cl are nearly consistent with those for other Mo(VI), Mo(V) and Mo(IV) species such as MoO_3, $Na_2MoO_4\cdot 2H_2O$, Al_2

$(MoO_4)_3$ and $CoMoO_4$ for Mo(VI), Mo_2O_5 for Mo(V), and MoO_2 for Mo(IV), respectively. In addition, a slight broadening of O 1s peak for Li_2FeMoO_4Cl is observed, which underlines that the oxygen ions in this compound are in different chemical environments one another due to the presence of mixed oxidation states of molybdenum in the lattice.

The amounts of Mo(VI), Mo(V) and Mo(IV) present in the Li_2FeMoO_4Cl lattice could be quantitatively estimated from the intensities of the corresponding deconvoluted spectrum and are approximately the same for one another. It is therefore concluded that Mo(VI) is reduced to thermodynamically unstable Mo(V) upon two moles of lithium intercalation, but there are two possible causes for the presence of Mo(VI) and Mo(IV); 1) disproportionation of Mo(V) producing Mo(VI) and Mo(IV), 2) the concentration gradient during lithium intercalation. In the latter case, it can be expected that the sample surface is probably enriched with Mo(IV) contents and the bulk with Mo (VI) ones. In the Mo 3d spectrum of Li_2FeMoO_4Cl before Ar ion sputtering, BE's are corresponding to Mo(VI) state, which is thought to result from reoxidation of Mo(V) or Mo(IV) at the pellet surface. On the other hand, there is no variation in the complex shape of Mo 3d spectra after 3 and 5 min. of Ar ion sputtering (a depth of 3 Å from the surface is etched by Ar ion sputtering).

Therefore, the two species, Mo(VI) and Mo(IV), could be considered as a result of the disproportionation of Mo(V). The emf of Mo species can be built up as follows:[14]

$$\text{Mo(VI)} \xrightarrow{+0.41} \text{Mo(V)} \xrightarrow{+0.73} \text{Mo(IV)}$$
$$\text{Mo(VI)} \xrightarrow{+0.57} \text{Mo(IV)}$$

It is not surprising that the pentavalent molybdenum ion is thermodynamically unstable with respect to disproportionation. Thus, upon further lithium intercalation, Mo(VI) in the lattice of $LiFeMoO_4Cl$ is previously reduced to Mo(V) instead of the reduction of iron (Fe(II) → Fe(0); electrode potential = −0.41 V). But, as mentioned above, the reduced Mo(V) ions undergo disproportionation to Mo(VI) and Mo(IV). The reason why the Mo(V) species coexist with Mo(VI) and Mo (IV) ones might be due to the fact that the formation of Mo(V) and its disproportionation reaction are in competition.

ACKNOWLEDGMENT. This work was supported by the Korean Ministry of Education (BSRI-94-3413) and we thank to C. Delmas for fruitful discussions.

REFERENCES

1. Choy, J. H.; Chang, S. H.; Noh, D. Y.; Son, K. A. *Bull. Korean Chem. Soc.* **1989**, *10*, 27.
2. Choy, J. H.; Noh, D. Y.; Son, K. A.; Seung, D. Y. *Bull. Korean Chem. Soc.* **1989**, *10*, 210.
3. Choy, J. H.; Noh, D. Y.; Park, J. C.; Chang, S. H.; Delmas, C.; Hagenmuller, P. *Mat. Res. Bull.* **1988**, *23*, 73.
4. Choy, J. H.; Noh, D. Y.; Chang, S. H.; Delmas, C. *Eur. J. Solid State Inorg. Chem.* **1990**, *t27*, 391.
5. Torardi, C. C.; Reiff, W. M.; Lazar, K.; Prince, E. *J. Phys. Chem. Solids* **1986**, *47*, 741.
6. Allen, G. C.; Curtis, M. T.; Hooper, A. T.; Tucker, P. M. *J. Chem. Soc. Dalton Trans.* **1974**, 1525.
7. Kishi, K.; Ikeda, S. *Bull. Chem. Soc. Jpn.* **1973**, *46*, 341.
8. McIntyre, N. S.; Zetaruk, D. G. *Anal. Chem.* **1977**, *49*, 1521.
9. Briggs, D.; Seah, M. P. *Practical Surface Analysis by Auger and X-ray Photoelectron Spectroscopy*; John Willey Sons: New York, 1983, pp 112-113.
10. Zingg, D. S.; Makovsky, L. E.; Tischer, R. E.; Brown, F. R.; Hercules, D. M. *J. Phys. Chem.* **1980**, *84*, 2898.
11. Grim, S. O.; Matienzo, L. J. *Inorg. Chem.* **1975**, *14*, 1014.
12. Lu, Y. C.; Clayton, C. R. *Corrosion Sci.* **1989**, *29*, 927.
13. Urgen, M.; Stolz, U.; Kirchheim, R. *Corrosion Sci.* **1990**, *30*, 377.
14. Bratsch, S. G. *J. Phys. Chem. Ref. Data* **1989**, *18*, 1.